Catal Lett
DOI 10.1007/s10562-016-1813-7

Organozirconium Complex with Keggin-Type Mono-Aluminum-Substituted Silicotungstate: Synthesis, Molecular Structure, and Catalytic Performance for Meerwein–Ponndorf–Verley Reduction

Chika Nozaki Kato[1,2] · Wataru Unno[1] · Sakie Kato[1] · Tsukasa Ogasawara[1] · Toshifumi Kashiwagi[1] · Hidemitsu Uno[3] · Kosuke Suzuki[4] · Noritaka Mizuno[4]

Received: 20 November 2015 / Accepted: 14 July 2016

Abstract The organozirconium complex with α-Keggin-type mono-aluminum-substituted silicotungstate, $[(n\text{-}C_4H_9)_4N]_6[\alpha\text{-}SiW_{11}Al(OH)_2O_{38}ZrCp_2]_2{\cdot}2H_2O$ (**TBA–Si–Al–Zr**) was synthesized by the reaction of $Cp_2Zr(OTf)_2{\cdot}THF$ (or Cp_2ZrCl_2) with $[(n\text{-}C_4H_9)_4N]_4K_{0.5}H_{0.5}[\alpha\text{-}SiW_{11}\{Al(OH_2)\}O_{39}]{\cdot}H_2O$ in acetonitrile. This compound showed high catalytic activities for Meerwein–Ponndorf–Verley reduction of ketones with 2-propanol in both homogeneous and heterogeneous system.

Graphical Abstract

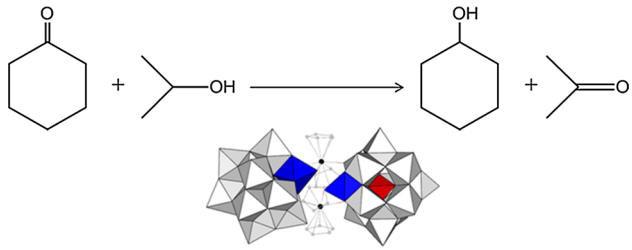

Keywords Organozirconium complex · Polyoxometalate · X-ray crystal structure · Meerwein–Ponndorf–Verley reduction · Heterogeneous catalyst

1 Introduction

Polyoxometalates (POMs) are discrete anionic metal–oxygen clusters that can be regarded as soluble oxide fragments. They have attracted substantial attention in the fields of catalysis, surface science, and materials science because of their chemical properties, including their redox potentials, acidities, and solubilities in various media, which can be finely tuned by choosing the appropriate constituent elements and countercations. In particular, the coordination of metal ions to the vacant site(s) of lacunary POMs is one of the most effective techniques for constructing efficient and well-defined active metal centers [1–4].

Several strategies for expanding POM chemistry have been considered, and covalent grafting reactions of organic/organometallic fragments onto the surfaces of POMs has been presented as an effective technique to functionalize POM-based materials [5–7]. For grafting

Electronic supplementary material The online version of this article (doi:10.1007/s10562-016-1813-7) contains supplementary material, which is available to authorized users.

✉ Chika Nozaki Kato
sckatou@ipc.shizuoka.ac.jp

[1] Department of Chemistry, Faculty of Science, Shizuoka University, 836 Ohya, Suruga-ku, Shizuoka 422-8529, Japan

[2] Green Chemistry Research Division, Research Institute of Green Science and Technology, Shizuoka University, 836 Ohya, Suruga-ku, Shizuoka 422-8529, Japan

[3] Department of Chemistry and Biology, Graduate School of Science and Engineering, Ehime University, Matsuyama 790-8577, Japan

[4] Department of Applied Chemistry, School of Engineering, The University of Tokyo, 7-3-1 Hongo, Bunkyo-ku, Tokyo 113-8656, Japan

Published online: 23 July 2016

reactions, complete (plenary) POMs obtained by the substitution of d^0 transition metals or reduction [5–16] and lacunary POM ligands [5–7, 17–24] have been used as supports, and numerous organic–inorganic hybrid materials have been applied to catalysts and functionalized materials. Thus, the development of polyoxoanion-supported organic/organometallic compounds has great potential to further expand POM chemistry.

To explore POMs that could be used as supports for grafting reactions, we focused on the aluminum-substituted POMs and successfully synthesized an organozirconium(IV)-supported polyoxometalate, [α-$PW_{11}Al(OH)O_{39}$-$ZrCp_2]_2^{6-}$ (Cp = η^5-$C_5H_5^-$) (**P–Al–Zr**), by a grafting reaction of α-Keggin mono-aluminum-substituted phosphotungstate with a bis(η^5-cyclopentadienyl)zirconium(IV) fragment [25]. Although the chemistry of organometallic moieties possessing η^5-cyclopentadienyl ligands has rapidly expanded [26–28], new studies on their grafting reactions onto POM surfaces have not been conducted: some examples (determined by X-ray analysis) include $\{[Cp_2U]_2(\mu\text{-}\kappa^2O\text{-}TiW_5O_{19})_2\}^{4-}$ [29, 30], $[(PW_{11}O_{39}NbO)_2ZrCp_2]^{6-}$ [31, 32], $[CpTiW_5O_{18}]^{3-}$ [33], $[Cp_3U(MW_5O_{19})_2]^{5-}$, and $[Cp_3Th(MW_5O_{19})_2]^{5-}$ (M = Nb, Ta) [34].

In this study, we focused on the use of the tetra-*n*-butylammonium/potassium salt of α-Keggin mono-aluminum-substituted silicotungstate, $[(n\text{-}C_4H_9)_4N]_4K_{0.5}H_{0.5}$[α-$SiW_{11}\{Al(OH_2)\}O_{39}]\cdot H_2O$ (**TBA–Si–Al**), as a support and synthesized the tetra-*n*-butylammonium salt of the organozirconium(IV) compound, $[(n\text{-}C_4H_9)_4N]_6$[α-$SiW_{11}Al(OH)_2O_{38}ZrCp_2]_2\cdot 2H_2O$ (**TBA–Si–Al–Zr**). The compound **TBA–Si–Al–Zr** was characterized by X-ray cry stallography, elemental analysis, TG/DTA, potentiometric titration, FTIR, cold-spray ionization mass (CSI-MS), and solution (^{27}Al, ^{1}H, and ^{13}C) and solid-state (^{27}Al, ^{13}C, and ^{29}Si) NMR spectroscopy. Furthermore, **TBA–Si–Al–Zr** and $[(n\text{-}C_4H_9)_4N]_6$[α-$PW_{11}Al(OH)O_{39}ZrCp_2]_2$ (**TBA–P–Al–Zr**) were used as homogeneous and heterogeneous catalysts in the Meerwein–Ponndorf–Verley(MPV) reduction of cyclohexanone, 2-hexanone, and cyclopentanone with 2-propanol. Herein, we report the complete details of the synthesis and molecular structure of complex **Si–Al–Zr** and demonstrate the catalytic activities of the bis(η^5-cyclopentadienyl)zirconium(IV) complexes with α-Keggin mono-aluminum-substituted polyoxotungstates.

2 Experimental

2.1 Materials

K_8[α-$SiW_{11}O_{39}]\cdot 12H_2O$ was synthesized according to the literature [35]. $[(n\text{-}C_4H_9)_4N]_4K_{0.5}H_{0.5}$[α-$SiW_{11}\{Al(OH_2)\}O_{39}]H_2O$ (**TBA–Si–Al**) was synthesized by a published method with modifications [36]. The synthesis and characterization results of **TBA–Si–Al** are shown in the Supporting Information. $H_3PW_{12}O_{40}23H_2O$ was obtained from Nippon Inorganic Colour & Chemical Co., Ltd (Japan). The number of solvated water molecules in these compounds was determined by TG/DTA analysis. **TBA–P–Al**, **TBA–P–Al–Zr**, and $Cp_2Zr(OTf)_2\cdot$THF (OTf = $CF_3SO_3^-$) were synthesized by previously published methods [25, 37]. All the reagents and solvents were obtained and used as received from commercial sources. Acetonitrile (containing ≤0.001 % water) was used for the synthesis of **TBA–Si–Al–Zr**.

2.2 Instrumentation/Analytical Procedures

Elemental analysis was performed using a Mikroanalytisches Labor Pascher (Remagen, Germany) instrument. The samples were dried overnight at room temperature under 10^{-3}–10^{-4} Torr vacuum before analysis. Infrared spectra were recorded on a Perkin Elmer Spectrum 100 FT-IR spectrometer, in KBr disks, at room temperature. Thermogravimetric (TG) and differential thermal analysis (DTA) data were obtained using a Rigaku Thermo Plus 2 series TG/DTA TG 8120. TG/DTA measurements were performed in air while increasing the temperature by 4 °C per min from 20 to 500 °C. Solution ^{1}H (600.17 MHz), ^{13}C (150.92 MHz), ^{31}P-{^{1}H} (242.95 MHz), ^{29}Si (119.23 MHz), and ^{27}Al NMR (156.36 MHz) spectra were recorded in 5-mm-outer diameter tubes on a JEOL ECA-600 NMR spectrometer. ^{1}H and ^{13}C NMR spectra were measured in acetonitrile-d_3 with reference to tetramethylsilane (TMS). Chemical shifts are reported as positive for resonances downfield of TMS (δ 0). The ^{31}P, ^{29}Si, and ^{27}Al NMR spectra were measured in acetonitrile-d_3 with reference to an external standard (a substitution method) of 85 % H_3PO_4 in a sealed capillary, TMS, and a saturated $AlCl_3$–D_2O solution, respectively. Chemical shifts for ^{31}P and ^{29}Si NMR spectra were reported as negative on the δ scale for resonances upfield of H_3PO_4 (δ 0) and TMS (δ 0). The chemical shifts in the ^{27}Al NMR spectra were reported as positive on the δ scale for resonances downfield of $AlCl_3$ (δ 0). When a quartz tube was used for ^{27}Al NMR spectroscopy, a background signal was also observed in the spectrum. Solid-state ^{27}Al, ^{13}C, and ^{29}Si NMR spectra were recorded at 400 MHz on a JEOL JNM-ECA 400 FT-NMR spectrometer with a JEOL ECP-400 NMR data-processing system. The chemical shifts δ for ^{27}Al and ^{13}C NMR spectra were reported to be positive on the δ scale for resonances upfield of $AlCl_3$ (δ 0) and the methyl group of $C_6(CH_3)_6$ (δ 17.4). The ^{29}Si NMR chemical shifts are reported as negative relative to polydimethylsilane (δ −31.0). Cold-spray ionization mass spectra (CSI-MS) were recorded on a JEOL JMS-T100CS (acetonitrile, 1 mg/mL; spray temperature, −20 °C) at The University of Tokyo.

Potentiometric titration was carried out with 0.010 mol/L tetra-*n*-butylammonium hydroxide as a titrant under Ar atmosphere [38]. The compound **TBA–Si–Al–Zr** (0.010 mmol) was dissolved in acetonitrile (20 mL) at 25 °C, and the solution was stirred for approximately 5 min. The titration data were obtained with a pH meter (Mettler Toledo). Data points were obtained in millivolt. A solution of tetra-*n*-butylammonium hydroxide (0.010 mol/L) was syringed into the suspension in 0.10-equivalent intervals.

2.3 Synthesis of $[(n\text{-}C_4H_9)_4N]_6[\alpha\text{-}SiW_{11}Al(OH)_2O_{38}ZrCp_2]_2{\cdot}2H_2O$ (TBA–Si–Al–Zr)

The following manipulations were performed in a dry box filled with Ar (>99.9995 vol% purity). A solution of $Cp_2Zr(OTf)_2{\cdot}THF$ (0.327 g; 0.54 mmol) dissolved in 10 mL of acetonitrile was slowly added to a solution of **TBA–Si–Al** (2.0 g; 0.54 mmol) dissolved in 15 mL of acetonitrile. The color of the solution changed to yellow. After stirring for 4 h at 25 °C, the mixed solution was filtered through a folded filter paper (Whatman #5). At this stage, the filtrate was removed from the dry box, and combined with water (400 mL) under ambient atmosphere. The yellow–white precipitate was collected using a membrane filter (JG 0.2 μm) and washed with a small amount of ethanol. The yield of the crude product was 1.721 g. The crude product (1.721 g) was dissolved in acetonitrile (34 mL) and then filtered through a folded filter paper (Whatman #5). The yellow platelet crystals were obtained by vapor diffusion from methanol in air. The yield of the product was 0.836 g (the percentage yield of 21.3 % was calculated based on the following: 2[moles of **TBA–Si–Al–Zr**]/[moles of **TBA–Si–Al**] × 100). Elemental analysis results showed: C, 19.02, H, 3.30; Al, 0.79; N, 1.15; Si, 0.75; W, 54.50; Zr, 2.45; K <0.01 %. Calculations for $[(n\text{-}C_4H_9)_4N]_6[\alpha\text{-}SiW_{11}A(OH)_2O_{38}ZrCp_2]_2{\cdot}2H_2O = C_{116}H_{244}Al_2N_6O_{82}Si_2W_{22}Zr_2$ (7372.267): C, 18.90, H, 3.34; Al, 0.73; N, 1.14; Si, 0.76; W, 54.86; Zr, 2.47; K 0 %. A weight loss of 0.18 % was observed during drying overnight at room temperature, under a vacuum of 10^{-3}–10^{-4} Torr prior to analysis, suggesting the removal of weakly solvated or adsorbed acetonitrile molecules; this was also supported by the absence of any signal attributable to acetonitrile molecules in the ^{1}H NMR spectrum of the sample acquired in DMSO-d_6 after drying overnight. TG/DTA performed under atmospheric conditions showed a weight loss of 24.74 % with exothermic points at 352.0 and 483.0 °C (observed below 500 °C). No clear endothermic point was observed. The calculated weight loss of 25.4 % was consistent with the loss of four Cp ligands, six tetra-*n*-butylammonium ions, and two water molecules. IR (KBr disk) in the 1300–400 cm^{-1} region (polyoxometalate region): 1012, 969, 921, 885, 799, 756, 733 s, and 669 m cm^{-1}. Solution NMR results gave ^{1}H NMR (CD_3CN, 25.4 °C): δ 6.69 (singlet) (Cp), 6.64 (singlet) (Cp), 6.63 (singlet) (Cp), 6.59 (singlet) (Cp), 3.16 (triplet), 1.65 (multiplet), 1.42 (multiplet), 1.00 (triplet) ($[(n\text{-}C_4H_9)_4N]^+$), and 2.15 (singlet) (H_2O); ^{13}C NMR (CD_3CN, 26.7 °C): δ 117.1 (Cp), 117.0 (Cp), 116.8 (Cp), 116.5 (Cp), 59.44, 24.51, 20.48, and 14.04 ($[(n\text{-}C_4H_9)_4N]^+$); ^{27}Al NMR (CD_3CN, 21.9 °C): δ 15.5. Solid NMR results gave ^{13}C NMR: δ 116.2 (singlet) (Cp), 58.6, 24.8, 20.5, and 14.8 ($[(n\text{-}C_4H_9)_4N]^+$); ^{27}Al NMR: δ 9.84; ^{29}Si NMR: δ −81.9. Positive ion CSI-MS (CH_3CN, 253 K) *m*/*z* 3910.8 and 7577.4 (calcd *m*/*z* 3910.4 $[\{(n\text{-}C_4H_9)_4N\}_8\{SiW_{11}Al(OH)_2O_{38}ZrCp_2\}_2]^{2+}$ and 7577.4 $[\{(n\text{-}C_4H_9)_4N\}_7\{SiW_{11}Al(OH)_2O_{38}ZrCp_2\}_2]^{+}$).

2.4 X-ray Crystallography

A yellow platelet-shaped crystal of **TBA–Si–Al–Zr** (0.140 × 0.090 × 0.040 mm) was mounted on a MicroMount. Data were collected on a Rigaku VariMax instrument with Saturn connected to a multi-layer mirror using monochromated Mo Kα radiation (λ = 0.71075 Å) at 154 ± 1 K. Data were collected and processed using the CrystalClear for Windows software. The structural analysis was performed using the CrystalStructure for Windows software. The structure was solved using SHELXS-97 (direct methods) and refined using SHELXL-97 [39]. For the polyoxoanion **Si–Al–Zr**, 22 W atoms, 2 Zr atoms, 2 Si atoms, 2 Al atoms, and 80 O atoms were clearly identified, thereby clarifying the main features of the molecular structure of the polyoxometalate. The six tetra-*n*-butylammonium ions and two water molecules could not be modeled with disordered atoms. Accordingly, the residual electron density was removed using the SQUEEZE routine in PLATON [40].

2.5 Crystal Data for TBA–Si–Al–Zr

$C_{116}H_{244}Al_2N_6O_{82}Si_2W_{22}Zr_2$; M = 7372.47, *monoclinic*, space group *C*2/*c* (#15), $a = 25.252(8)$, $b = 17.619(6)$, $c = 46.77(2)$ Å, $V = 20807(11)$ Å^3, $Z = 4$, $D_c = 2.353$ g/cm^3, μ(Mo-Kα) 123.080 cm^{-1}. $R_1 = 0.0721$ ($I > 2\sigma(I)$), w$R_2 = 0.2308$ (for all data). GOF = 1.126 (100,607 total reflections, 21,524 unique reflections where $I > 2\sigma(I)$). Some acetonitrile molecules were observed in a single crystal of **TBA–Si–Al–Zr**; however, no acetonitrile solvent molecules were observed by elemental analysis or ^{1}H NMR spectroscopy. Thus, the solvent molecules evaporate gradually when crystals are removed from acetonitrile solution. CCDC reference number 967942. The data for **TBA–Si–Al–Zr** can be obtained free of charge at www.ccdc.cam.ac.uk/conts/retrieving.html [or from Cambridge Crystallographic Data Centre, 12 Union Road, Cambridge

CB2 1EZ, UK; Fax: +44-1223-336-033; E-mail: deposite@ccdc.cam.ac.uk.]

2.6 MPV Reduction

For the MPV reduction of cyclohexanone with 2-propanol in a homogeneous system, a sample catalyst was placed in a 60 mL Schlenk tube under Ar atmosphere. Cyclohexanone (1.9 mmol), 2-propanol (13 mmol), and acetonitrile (4 mL) were added using a micropipette. In a heterogeneous system, a mixture of catalyst, ketones (cyclohexanone, cyclopentanone, and 2-hexanone; 1.6–2.2 mmol), and 2-propanol (78 mmol) was placed in a Schlenk tube under Ar atmosphere. The reaction mixture was heated in an oil bath at 80 ± 2 °C. The reaction solution was analyzed by gas chromatography (flame ionization detector, a capillary column DB-WAX, 0.53 mm × 15 m and a glass column BX-10, 3.2 mm × 3 m) and ^{1}H NMR spectroscopy. Values of the products were assigned by comparing the obtained results with the analysis results obtained from analyzing the authentic samples under the same conditions. The conversion (%) and turnover number (TON) was calculated as $\{[\text{mol of substrate}]_0 - [\text{mol of substrate}]_t\}/[\text{mol of substrate}]_0 \times 100$ and $[\text{mol of corresponding alcohol}]_t/[\text{mol of catalyst}]$, respectively.

3 Results and Discussion

3.1 Synthesis and molecular structure of $[(n\text{-}C_4H_9)_4N]_6[\alpha\text{-}SiW_{11}Al(OH)_2O_{38}ZrCp_2]_2\cdot 2H_2O$ (TBA–Si–Al–Zr)

The bis(η^5-cyclopentadienyl)zirconium(IV) compound with α-Keggin mono-aluminum-substituted silicotungstate **Si–Al–Zr** was obtained in 21.3 % yield based on the tetra-*n*-butylammonium salt $[(n\text{-}C_4H_9)_4N]_6[\alpha\text{-}SiW_{11}Al(OH)_2O_{38}ZrCp_2]_2\cdot 2H_2O$ (**TBA–Si–Al–Zr**). This compound was prepared by the 1:1 stoichiometric reaction of $[(n\text{-}C_4H_9)_4N]_4K_{0.5}H_{0.5}[\alpha\text{-}SiW_{11}\{Al(OH_2)\}O_{39}]\cdot H_2O$ (**TBA–Si–Al**) with $Cp_2Zr(OTf)_2\cdot$THF in acetonitrile under an Ar atmosphere, followed by precipitation from water under ambient atmosphere. Finally, yellow crystalline products were obtained by crystallization via vapor diffusion from acetonitrile/methanol at 25 °C in air. When $Cp_2Zr(OTf)_2$-THF was added to the acetonitrile solution of $H_3PW_{12}O_{40}\cdot 23H_2O$, a white precipitate formed and it was insoluble in acetonitrile. It was noted that polyoxoanion **Si–Al–Zr** was formed by the direct reaction of **TBA–Si–Al** with Cp_2ZrCl_2 in air, whereas the polyoxoanion **P–Al–Zr** was not obtained by a direct reaction of $[\alpha\text{-}PW_{11}\{Al(OH_2)\}O_{39}]^{4-}$ (**P–Al**) with zirconocene dichloride. In addition, single crystals suitable for X-ray crystallography of **TBA–Si–Al–Zr** were quite stable toward moisture; in contrast, the quality of **TBA–P–Al–Zr** crystals degrades gradually upon exposure to moisture. Thus, the internal Si and P atoms in polyoxoanions markedly affected the reactivity with zirconocene dichloride and the resulting stability toward moisture.

Elemental analysis of **TBA–Si–Al–Zr** dried overnight at room temperature under 10^{-3}–10^{-4} Torr of vacuum prior to analysis was consistent with the composition $[(n\text{-}C_4H_9)_4N]_6[\alpha\text{-}SiW_{11}Al(OH)_2O_{38}ZrCp_2]_2\cdot 2H_2O$. The weight loss observed during the drying of **TBA–Si–Al–Zr** prior to analysis was 0.18 %, suggesting the absence of solvent molecules. This suggestion was also supported by the ^{1}H NMR spectrum, as shown in the Experimental section. A weight loss of 25.4 % with exothermic points at 352.0 and 483.0 °C was observed from 17.5 to 500 °C in the TG/DTA performed under atmospheric conditions; calculations based on these data indicated the loss of six $[(n\text{-}C_4H_9)_4N]^+$ (calcd. 19.7 %) and four cyclopentadienyl groups (calcd. 3.5 %) (total: 23.2 %).

X-ray structural analysis revealed that the polyoxoanion **Si–Al–Zr** is dimeric, containing two $\{SiW_{11}AlO_{40}\}$ units bridged by two "bent sandwich" Cp_2Zr^{2+} fragments, as shown in Fig. 1. Selected bond distances and angles around the Zr center in **Si–Al–Zr** are summarized in Table 1, and the bond valence sum (BVS) calculations of the W, Si, Al, and O atoms (Table S1) are provided in the Supporting Information. Each Zr center was bound to the terminal O atoms of the Al and W sites and to the edge-sharing O atom of the Al–O–W linkage with 5-coordination geometry. The molecular structure of **Si–Al–Zr** was quite similar to that of **P–Al–Zr**; however, the Al···Al (5.47 Å) distance was larger than that of the polyoxoanion **P–Al–Zr** (5.32 Å), and the angles of the Al–O–Zr bond (109.7°), the O–Zr–O bond (73.5°), and the W–O–Zr bond (163.6°) were larger than those of the polyoxoanion **P–Al–Zr** (105.3°, 69.1°, and 159.7°, respectively). Thus, the two $\{SiW_{11}AlO_{40}\}$ units were displaced from each other relative to those of the polyoxoanion **P–Al–Zr**.

The values of the bond valence sums (BVSs) for **TBA–Si–Al–Zr** [41–44], which were calculated based on the observed bond lengths, were in the range of 5.615–6.107 (average 5.861) for the 11 W atoms, 4.067 for the one Si atom, 2.712 for the one Al atom, and in the range of 1.623–2.063 (average 1.842) for the 38 O atoms, excluding O(18) and O(21); these values were in reasonable agreement with the formal valences of W^{6+}, Si^{4+}, Al^{3+}, and O^{2-}, respectively (Table S1). The calculated BVS values of O(18) and O(21) at the Al–O–Zr and Al–O–W linkages were 1.033 and 1.249, respectively, suggesting that a pair of protons were bound to each of the two bridging O atoms between the Al and Zr atoms, and another pair of protons was bound to the two bridging O atoms between the Al and W atoms. From the potentiometric titration, three break points at 2, 3, and 4 equivalents of added base were

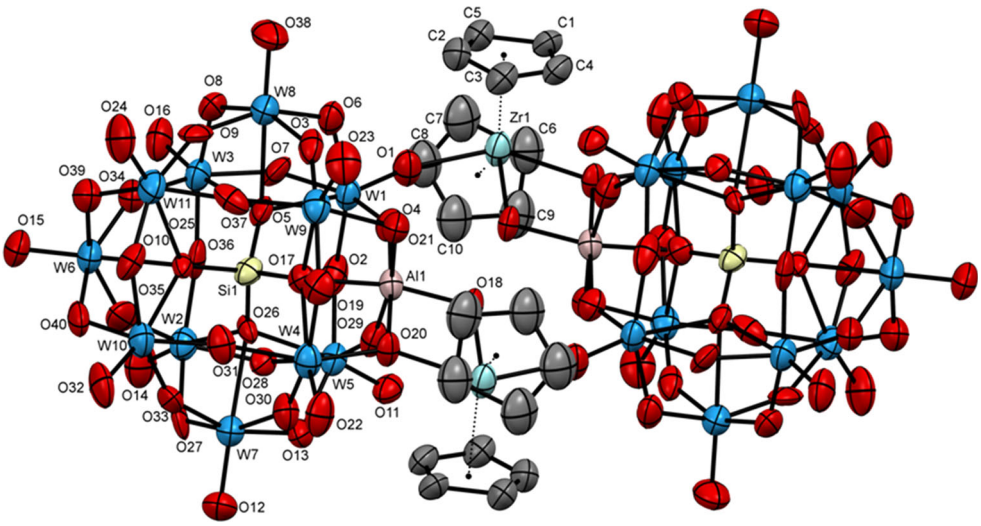

Fig. 1 Molecular structure of polyoxoanion **Si–Al–Zr** with atom numberings

Table 1 Selected bond distances and angles around zirconium and aluminum sites in **TBA–Si–Al–Zr**

Distances (Å)			
Al(1)–O(4)	1.865 (11)	W(1)–O(1)	1.748 (10)
Al(1)–O(17)	2.035 (10)	W(1)–O(2)	1.919 (12)
Al(1)–O(18)	1.873 (9)	W(1)–O(4)	1.831 (10)
Al(1)–O(20)	1.948 (10)	W(1)–O(5)	2.035 (9)
Al(1)–O(21)	1.903 (11)	W(1)–O(6)	1.949 (11)
Al(1)–O(29)	1.885 (11)	W(1)–O(7)	2.060 (10)
Zr(1)–O(1)	2.230 (10)	W(4)–O(17)	2.397 (9)
Zr(1)–O(18)[a]	2.164 (10)	W(4)–O(19)	1.930 (11)
Zr(1)–O(20)[a]	2.239 (9)	W(4)–O(20)	1.933 (8)
Si(1)–O(17)	1.635 (10)	W(4)–O(22)	1.715 (11)
Zr(1)···Zr(1)	7.950 (3)	W(4)–O(30)	1.916 (10)
Al(1)···Al(1)	5.465 (5)	W(4)–O(31)	1.959 (10)
Zr(1)–centroid Cp(1–5)	2.273		
Zr(1)–centroid Cp(6–10)	2.264		
Angles (°)			
Al(1)–O(18)–Zr(1)[a]	109.7 (5)	W(1)–O(1)–Zr(1)	163.5 (6)
O(1)–Zr(1)–O(18)[a]	73.5 (4)	W(1)–O(4)–Al(1)	145.3 (6)
O(18)–Al(1)–O(20)	79.1 (4)	O(1)–W(1)–O(4)	100.7 (5)
Cp(1–5)–Zr(1)–Cp(6–10)	128.92		

[a] Symmetry operator: (1) −X+1/2+1, −Y+1/2+1, −Z+1

observed, as shown in Figure S1. This result also supported the presence of four protons in **Si–Al–Zr**.

The FTIR spectra acquired in the POM region of **TBA–Si–Al–Zr** and **TBA–Si–Al** from KBr disks of the compounds are presented in Fig. 2. The IR spectrum of **TBA–Si–Al–Zr** (1012, 969, 921, 885, 799, 756, 733, and 669 cm^{-1}) was different from that of **TBA–Si–Al** (1006, 960, 916, 880, 799, and 740 cm^{-1}). Specifically, a new band appeared at 669 cm^{-1}, probably because of the formation of Zr–O linkages; this was observed at 631 cm^{-1} for **TBA–P–Al–Zr** [25]. A band assigned to the Cp ligands was clearly observed at 3121 cm^{-1}. These results suggested that the η^5-cyclopentadienylzirconium fragments were coordinated to the $[\alpha\text{-SiW}_{11}\{Al(OH_2)\}O_{39}]^{5-}$ surface.

The cold-spray ionization mass (CSI-MS) spectrum of **TBA–Si–Al–Zr** in acetonitrile exhibited peaks at $m/z = 3910.8$ and 7577.4, as shown in Fig. 3. These peaks were assigned to $[\{(n\text{-}C_4H_9)_4N\}_8\{SiW_{11}Al(OH)_2O_{38}Zr Cp_2\}_2]^{2+}$ and $[\{(n\text{-}C_4H_9)_4N\}_7\{SiW_{11}Al(OH)_2O_{38}Zr Cp_2\}_2]^{+}$, respectively, clearly indicating that the dimeric structure of **Si–Al–Zr** was maintained in acetonitrile solution.

The solution ^{27}Al NMR spectra of **TBA–Si–Al–Zr** and **TBA–Si–Al** acquired at 25 °C in acetonitrile-d_3 are shown in Figs. 4 and S2. **TBA–Si–Al–Zr** showed a signal at 15.5 ppm, which was shifted relative to that of **TBA–Si–Al** (δ 16.0). The solid-state ^{27}Al NMR spectrum of **TBA–Si–Al–Zr** also showed a signal at 9.8 ppm, as shown in Figure S3. These results indicated that the η^5-cyclopentadienylzirconium fragment was grafted on the surface of **Si–Al** and that the two Al sites in the $\{SiW_{11}AlO_{40}\}$ unit were equivalent in both the solution and solid phases. The solution ^{29}Si NMR spectrum was not obtained because of the low solubility of **TBA–Si–Al–Zr** in acetonitrile. The solid-state ^{29}Si NMR spectrum of **TBA–Si–Al–Zr** was quite noisy; however, a signal was observed at −81.9 ppm (Figure S4). This also confirmed that the two $\{SiW_{11}AlO_{40}\}$ units were equivalent.

The ^{1}H NMR spectrum (Fig. 5a) of **TBA–Si–Al–Zr** obtained at ∼25 °C in acetonitrile-d_3 showed four signals at 6.69, 6.64, 6.63, and 6.59 ppm, with an integrated intensity ratio of approximately 1:1:1:1; these peaks were shifted relative to those of $Cp_2Zr(OTf)_2{\cdot}THF$ (δ 6.52). No

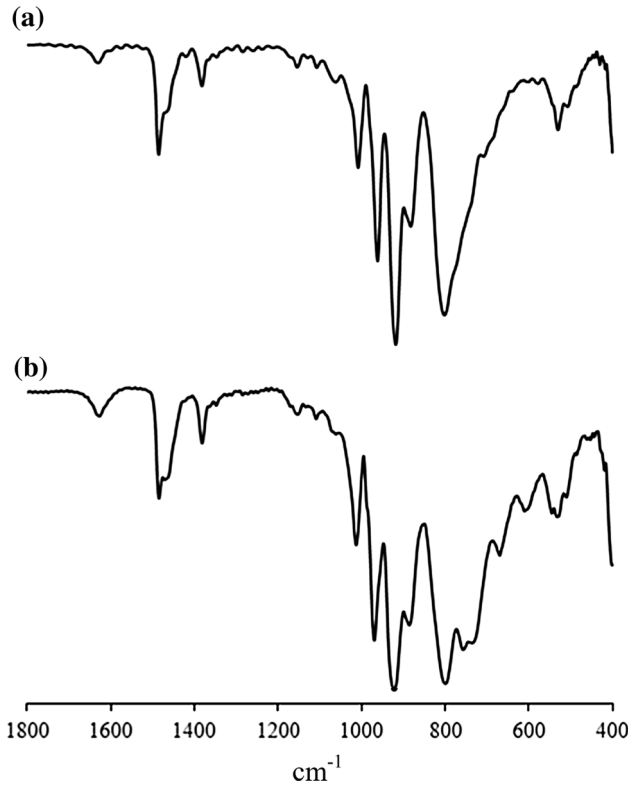

Fig. 2 FTIR spectra in the polyoxoanion region (1800–400 cm^{-1}), as acquired from KBr disk of **a TBA–Si–Al** and **b TBA–Si–Al–Zr**

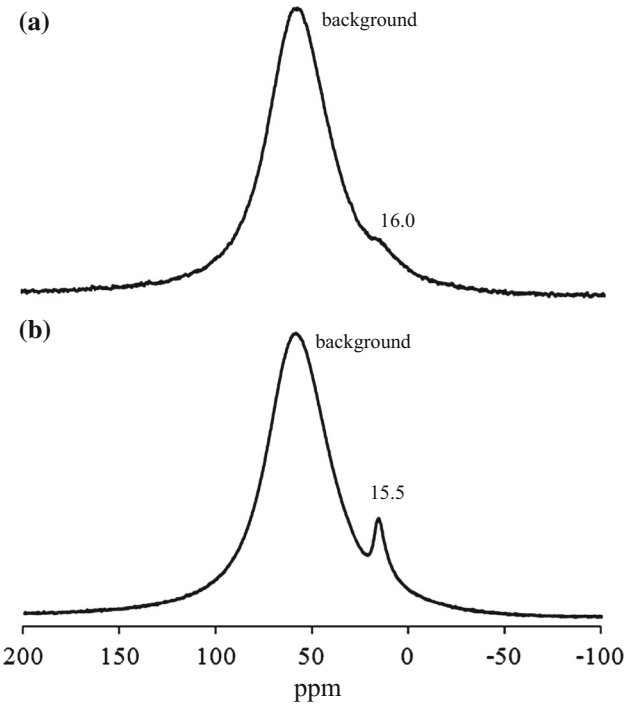

Fig. 4 ^{27}Al NMR spectra in acetonitrile-d_3 of **a TBA–Si–Al** and **b TBA–Si–Al–Zr**

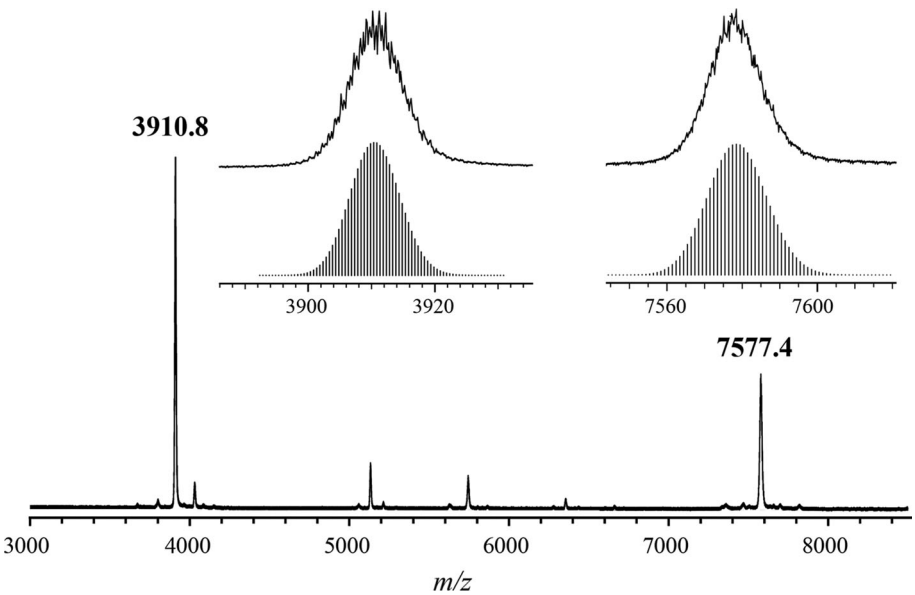

Fig. 3 CSI-MS spectrum of the acetonitrile solution of **TBA–Si–Al–Zr**. *Inset* spectra in the range of *m/z* 3890–3930 and 7550–7620, and the calculated patterns for $[\{(n\text{-}C_4H_9)_4N\}_8\{SiW_{11}Al(OH)_2O_{38}Zr Cp_2\}_2]^{2+}$ (*m/z* 3910.8) and $[\{(n\text{-}C_4H_9)_4N\}_7\{SiW_{11}Al(OH)_2O_{38}Zr Cp_2\}_2]^{+}$ (*m/z* 7577.4)

signal attributable to the Cp_2Zr^{2+} (δ 6.44) formed by the reaction of Cp_2ZrCl_2 with $AgBF_4$ was observed in acetonitrile-d_3, suggesting that the Cp_2Zr^{2+} fragments were not eliminated from the surface of $[\alpha\text{-}SiW_{11}\{Al(OH_2)\}O_{39}]^{5-}$ (**Si–Al**). Four signals were observed in the ^{13}C NMR spectrum at 117.1, 117.0, 116.8, and 116.5 ppm

(Fig. 5b). In contrast, the solid-state ^{13}C NMR spectrum of **TBA–Si–Al–Zr** showed a signal at 116.2 ppm that was ascribed to Cp ligands, as shown in Fig. 6. Thus, the four Cp ligands were not equivalent in acetonitrile solution whereas they were equivalent in the solid phase.

3.2 Meerwein–Ponndorf–Verley(MPV) Reduction of Ketones with 2-propanol Catalyzed by TBA–Si–Al–Zr and TBA–P–Al–Zr in Homogeneous and Heterogeneous Systems

First of all, the hydrogen-transfer reaction between cyclohexanone and 2-propanol at 80 ± 2 °C catalyzed by **TBA–Si–Al–Zr** and **TBA–P–Al–Zr** was examined in a homogeneous system, as shown in Fig. 7. The catalytic activities are summarized in Table 2. During the reduction reactions, all the catalysts in Table 2 were soluble in acetonitrile. Cyclohexanol and acetone were obtained with >99 % selectivity. No reaction was observed in the absence of a catalyst under the tested reaction conditions. A Brønsted acid catalyst, $H_3PW_{12}O_{40}{\cdot}23H_2O$, also showed no reaction. The conversions involving both **TBA–Si–Al–Zr** and **TBA–P–Al–Zr** were >99 % complete after 24 h and both turnover numbers (TON = [mol of cyclohexanol]/[mol of catalyst]) reached 280. As control experiments, **TBA–Si–Al** and $[(n\text{-}C_4H_9)_4N]_4[\alpha\text{-}PW_{11}\{Al(OH_2)\}O_{39}]$ (**TBA–P–Al**) showed no reaction within 24 h. The conversions of Cp_2ZrCl_2 and a mixture of Cp_2ZrCl_2 and **TBA–P–Al** after 24 h were 1.7 and 0.95 %, respectively; this supported the result that **TBA–P–Al–Zr** was not obtained by a direct reaction of **TBA–P–Al** with Cp_2ZrCl_2, as mentioned above. In contrast, **TBA–Si–Al–Zr** was easily formed by the reaction of **TBA–Si–Al** with Cp_2ZrCl_2 in acetonitrile, and showed the high catalytic activities. Thus, the grafting reaction of Cp_2ZrCl_2 onto the mono-aluminum-substituted site in **TBA–Si–Al** caused the effective active centers. Here, $Cp_2Zr(OTf)_2THF$ showed faster initial rates, as shown in Figure S5. The conversion after 3 h was 29 %, exceeding those of **TBA–Si–Al–Zr** (18 %) and **TBA–P–Al–Zr** (20 %), and after 24 h, the conversion was 82 % (TON was 116). When TON was calculated on the basis of [mol of cyclohexanol]/[mol of zirconium atom], both TON after 24 h of **TBA–Si–Al–Zr** and **TBA–P–Al–Zr** was 140, which was similar order to that of $Cp_2Zr(OTf)_2THF$ (116). Thus, a clear effect of grafting reactions of $Cp_2Zr(OTf)_2$-THF onto the mono-aluminum-substituted sites in **TBA–Si–Al–Zr** and **TBA–P–Al–Zr** was not observed under the present reaction conditions.

However, **TBA–Si–Al–Zr** and **TBA–P–Al–Zr** can be used as heterogeneous catalysts because they are insoluble in 2-propanol; while, $Cp_2Zr(OTf)_2{\cdot}THF$ is soluble in 2-propanol. The catalytic activities of **TBA–Si–Al–Zr** and **TBA–P–Al–Zr** in a heterogeneous system, i.e., in the absence of acetonitrile, were investigated for the MPV reduction of cyclohexanone, cyclopentanone, and 2-hexanone with 2-propanol at 80 ± 2 °C, as shown in Table 3. For the all reactions, the corresponding alcohols and acetone were formed with >99 % selectively. For the reaction

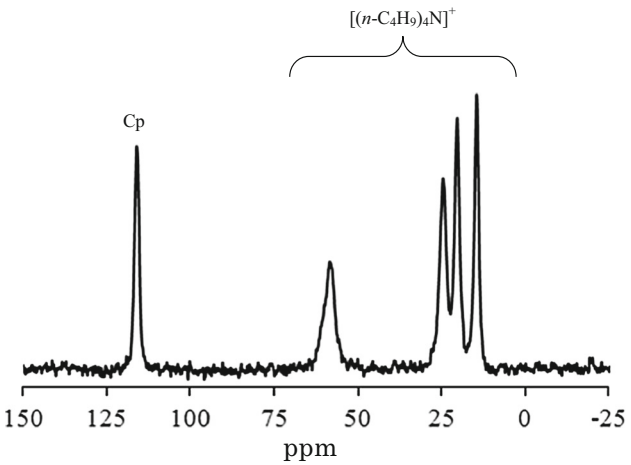

Fig. 6 Solid-state ^{13}C NMR spectrum of **TBA–Si–Al–Zr**

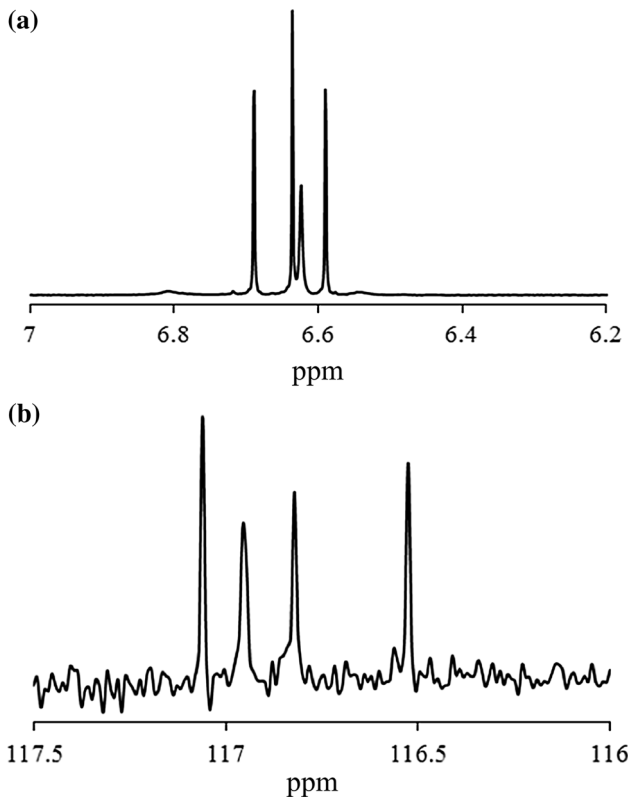

Fig. 5 **a** ^{1}H NMR and **b** ^{13}C NMR spectra in acetonitrile-d_3 of **TBA–Si–Al–Zr**

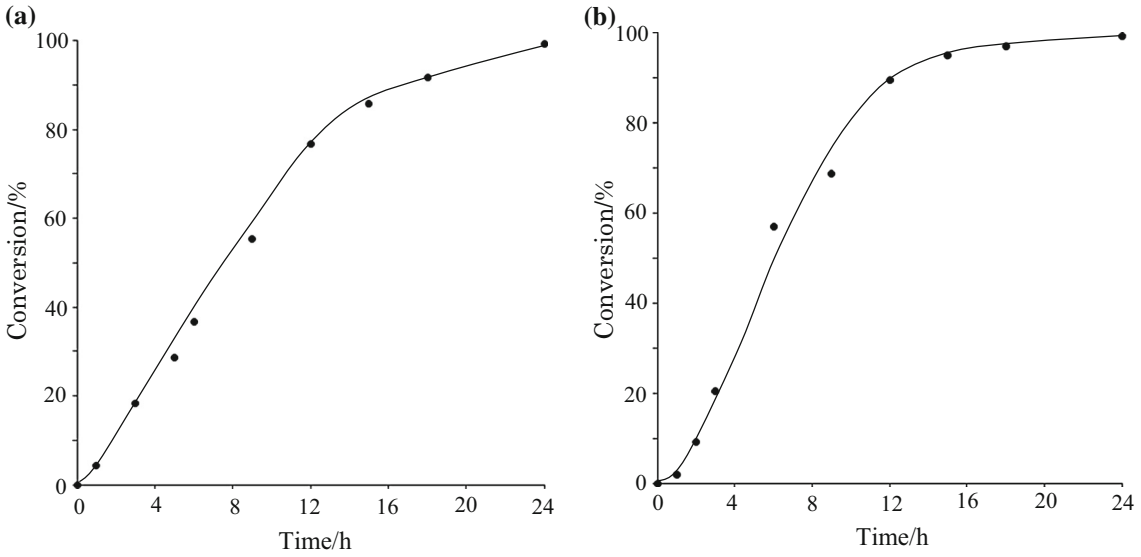

Fig. 7 Time course for the Meerwein–Ponndorf–Verley reduction of cyclohexanone with 2-propanol catalyzed by **a TBA–Si–Al–Zr** and **b TBA–P–Al–Zr**. Reaction conditions: see Table 2

Table 2 Meerwein–Ponndorf–Verley reduction of cyclohexanone with 2-propanol in a homogeneous system

Catalyst (μmol)	Reaction time (h)	Selectivity of cyclohexanol (%)	TON[a]	Conversion (%)[b]
TBA–Si–Al–Zr (6.8)	3	>99	51	18
	24	>99	280	>99
TBA–P–Al–Zr (6.8)	3	>99	57	20
	24	>99	280	>99
$Cp_2Zr(OTf)_2THF$ (13.5)	3	>99	40	29
	24	>99	116	82
Cp_2ZrCl_2 (13.7)	24	>99	2.3	1.7
A mixture of **TBA–P–Al** (13.5) and Cp_2ZrCl_2 (13.7)	24	>99	1.3[c]	0.95
TBA–Si–Al (6.7)	24	–	–	–
TBA–P–Al (6.8)	24	–	–	–

Reaction conditions: catalyst (6.7–13.7 μmol), cyclohexanone (1.9 mmol), 2-propanol (13 mmol), acetonitrile (4 mL), reaction temperature 80 ± 2 °C, under argon

[a] Turnover number (TON) = [mol of cyclohexanol]$_t$/[mol of catalyst]

[b] Conversion (%) = {[mol of cyclohexanone]$_0$ − [mol of cyclohexanone]$_t$}/[mol of cyclohexanone]$_0$ × 100

[c] TON was calculated on the basis of mol of **TBA–P–Al**

of cyclohexanone, the conversion after 24 h of **TBA–Si–Al–Zr** reached >99 %; while, **TBA–P–Al–Zr** showed a low conversion (46 %). A numerous homogeneous and heterogeneous catalysts for MPV reduction have been reported [45, 46]. Some of the recent examples containing aluminum and zirconium, Cp_2ZrH_2 [47], ZrO_2 [48], zirconium 1-propoxide grafted on SBA-15 [49], porous zirconium-phytic acid hybrid [50], partially crystalline zirconosilicate [51], $[CH_2\{Me(Me_3Si)_2Si\}_2SiO]_2AlOPr^i$(-$HOPr^i$) [52], Mg/Al and Ca/Al mixed oxides [53, 54], and aluminum isopropoxide-grafted mesoporous organosilica [55], exhibited high conversions (>80 %) of cyclohexanone with 2-propanol under various reaction conditions. Although it is difficult to draw a simple comparison, the catalytic activities of **TBA–Si–Al–Zr** were by no means inferior to them in both homogeneous and heterogeneous system. **TBA–Si–Al–Zr** also showed the higher conversion (55 % after 96 h) in the MPV reduction of cyclopentanone than that of **TBA–P–Al–Zr** (30 %). When 2-hexanone was used as a substrate, the conversion after 96 h of **TBA–Si–Al–Zr** decreased to 24 %, which was similar to that of **TBA–P–Al–Zr** (26 %).

Table 3 Meerwein–Ponndorf–Verleyreduction of ketones with 2-propanol in a heterogeneous system

Substrate (mmol)	Catalyst	Reaction time (h)	Selectivity of product (%)	TON[a]	Conversion (%)[b]
Cyclohexanone (1.9)	**TBA–Si–Al–Zr**	24	Cyclohexanol (>99)	70	>99
	TBA–P–Al–Zr	24	Cyclohexanol (>99)	33	46
Cyclopentanone (2.2)	**TBA–Si–Al–Zr**	96	Cyclopentanol (>99)	45	55
	TBA–P–Al–Zr	96	Cyclopentanol (>99)	24	30
2-hexanone (1.6)	**TBA–Si–Al–Zr**	96	2-hexanol (>99)	14	24
	TBA–P–Al–Zr	96	2-hexanol (>99)	15	26

Reaction conditions: catalyst (27 μmol), substrates (1.6–2.2 mmol), 2-propanol (78 mmol), reaction temperature 80 ± 2 °C, under argon

[a] Turnover number (TON) = [mol of corresponding alcohol]$_t$/[mol of catalyst]

[b] Conversion (%) = {[mol of substrate]$_0$−[mol of substrate]$_t$}/[mol of substrate]$_0$ × 100

After 24 h of reaction for cyclohexanone, the catalysts were collected using a membrane filter (JG 0.2 μm) and washed with a small amount of ethanol. No precipitation was formed by the addition of excess water to the filtrates, suggesting no leaching of **TBA–Si–Al–Zr** and **TBA–P–Al–Zr** into the reaction solutions. ^{31}P NMR spectrum in acetonitrile-d_3 of the filtrate of **TBA–P–Al–Zr** also showed no signals; this suggested that **TBA–P–Al–Zr** did not leach into the solutions. The FT-IR spectra of solid samples showed bands at (1010, 965, 921, 883, 800, 758, and 668 cm^{-1}) and (1080, 1065, 969, 888, 810, 786, 749, 703, and 629 cm^{-1}), respectively, which were the same as those of as-prepared samples [25]. The ^{31}P NMR spectrum in acetonitrile-d_3 of a solid sample of **TBA–P–Al–Zr** also showed two signals at −12.25 and −12.35 ppm, which were the same as those of as-prepared sample [25]. No other signals were observed. These results suggested that the dimeric structures of **TBA–Si–Al–Zr** and **TBA–P–Al–Zr** were maintained under the present reaction conditions. For the ^{1}H NMR spectrum in acetonitrile-d_3 of a sample of **TBA–Si–Al–Zr**, four signals assigned to Cp ligands were observed at 6.69, 6.64, 6.63, and 6.59 ppm, which were the same as those of as-prepared sample (Figure S8a). The ^{1}H NMR spectrum of a sample of **TBA–P–Al–Zr** showed two signals of Cp ligands at 6.67 and 6.56 ppm, as shown in Figure S8b. The two signals were also the same as those of as-prepared sample [25]. Thus, the active centers would not be caused by cleavage of linkages between the two Keggin mono-aluminum-substituted units. When a solid sample of **TBA–Si–Al–Zr** was used as a catalyst in the second run for the MPV reduction of cyclohexanone with 2-propanol at 80 ± 2 °C, the conversion after 24 h was approximately 90 %, showing that **TBA–Si–Al–Zr** was basically recyclable. Further studies regarding the reaction mechanism including determination of the active centers are in progress and will be reported elsewhere.

4 Conclusion

The tetra-*n*-butylammonium salt of [α-$SiW_{11}Al(OH)_2O_{38}$-$ZrCp_2]_2^{6-}$ (**Si–Al–Zr**), [$(n$-$C_4H_9)_4N]_6$[α-$SiW_{11}Al(OH)_2$-$O_{38}ZrCp_2]_2$·$2H_2O$ (**TBA–Si–Al–Zr**), was obtained from a 1:1 stoichiometric reaction of [$(n$-$C_4H_9)_4N]_4K_{0.5}H_{0.5}$[α-$SiW_{11}${$Al(OH_2)$}$O_{39}$]·$H_2O$ (**TBA–Si–Al**) with Cp_2-$Zr(OTf)_2$·THF in acetonitrile solution under an Ar atmosphere, followed by precipitation from water and crystallization via vapor diffusion from acetonitrile/methanol in air. Single-crystal X-ray structure analysis of **TBA–Si–Al–Zr** revealed that the two {$SiW_{11}AlO_{40}$} units are bridged by two "bent sandwich" Cp_2Zr^{2+} fragments, in which the four η^5-cyclopentadienyl ligands were equivalent in the solid phase but not equivalent in acetonitrile solution. The molecular structure of **Si–Al–Zr** was quite similar to that of [α-$PW_{11}Al(OH)O_{39}ZrCp_2]_2^{6-}$ (**P–Al–Zr**); however, the partial structures around Al and Zr centers, including the position and number of protons, and the dynamic behaviors of the four Cp ligands in acetonitrile solution were remarkably different from those of **P–Zr–Al**. **TBA–Si–Al–Zr** was also formed by a 1:1 stoichiometric reaction of **TBA–Si–Al** with Cp_2ZrCl_2 in air; this was different from that of [$(n$-$C_4H_9)_4N]_6$[α-$PW_{11}Al(OH)O_{39}$-$ZrCp_2]_2$ (**TBA–P–Al–Zr**). Furthermore, we investigated the catalytic activities of **TBA–Si–Al–Zr** and **TBA–P–Al–Zr** in the MPV reduction of cyclohexanone, cyclopentanone, and 2-hexanone with 2-propanol in both homogeneous and heterogeneous system. In a homogenous system, both compounds exhibited >99 % conversions after 24 h for the MPV reduction of cyclohexanone; thus, a clear effect of the internal atoms was not observed. In contrast, **TBA–Si–Al–Zr** exhibited the higher activities than those of **TBA–P–Al–Zr** for cyclohexanone and cyclopentanone in a heterogeneous system. FT-IR and ^{31}P NMR spectra showed that the dimeric structures of these compounds were maintained under the present reaction conditions. Thus, the direct reaction of $Cp_2Zr(OTf)_2$THF (or

Cp_2ZrCl_2) with **TBA–Si–Al–Zr** caused the high catalytic activities for MPV reduction in both homogeneous and heterogeneous system.

Acknowledgments This work was supported by a Grant-in-Aid for Scientific Research of the Ministry of Education, Culture, Sports, Science and Technology of Japan.

References

1. Pope MT (1983) Heteropoly and isopoly oxometalates. Springer-Verlag, Berlin
2. Pope MT, Müller A (1991) Angew Chem Int Ed Engl 30:34
3. Pope MT, Müller A (eds) (1994) Polyoxometalates: from platonic solids to anti-retroviral activity. Kluwer Academic Publishers, Dordrecht
4. Wang S, Yang G (2015) Chem Rev 115:4893
5. Dolbecq A, Dumas E, Mayer CR, Mialane P (2010) Chem Rev 110:6009
6. Dolbecq A, Mialane P, Sècheresse F, Keita B, Nadjo L (2012) Chem Commun 48:8299
7. Proust A, Thouvenot R, Gouzerh P (2008) Chem Commun 16:1837
8. Gouzerh P, Proust A (1998) Chem Rev 98:77
9. Day VW, Klemperer WG (1993) Mol Eng 3:61
10. Day VW, Eberspacher TA, Klemperer WG, Planalp RP, Schiller PW, Yagasaki A, Zhong B (1993) Inorg Chem 32:1629
11. Day VW, Klemperer WG, Main DJ (1990) Inorg Chem 29:2345
12. Klemperer WG, Main DJ (1990) Inorg Chem 29:2355
13. Weiner H, Hayashi Y, Finke RG (1999) Inorg Chem 38:2579
14. Nomiya K, Mizuno N, Lyon DK, Phol M, Finke RG (1997) Inorg Synth 31:186
15. Lin Y, Nomiya K, Finke RG (1993) Inorg Chem 32:6040
16. Rapko BM, Pohl M, Finke RG (1994) Inorg Chem 33:3625
17. Yang L, Hou L, Ma P, Niu J (2013) J Coord Chem 66:1330
18. Laurencin D, Villanneau R, Gérard H, Proust A (2006) J Phys Chem A 110:6345
19. Artero V, Laurencin D, Villanneau R, Thouvenot R, Herson P, Gouzerh P, Proust A (2005) Inorg Chem 44:2826
20. Sakai Y, Shinohara A, Hayashi K, Nomiya K (2006) Eur J Inorg Chem 1:163
21. Nomiya K, Hayashi K, Kasahara Y, Iida T, Nagaoka Y, Yamamoto H, Ueno T, Sakai Y (2007) Bull Chem Soc Jpn 80:724
22. Kato CN, Morii Y, Hattori S, Nakayama R, Makino Y, Uno H (2012) Dalton Trans 41:10021
23. Dupré N, Brazel C, Fensterbank L, Malacria M, Thourimbert S, Hasenknopf B, Lacôte E (2012) Chem Eur J 18:12962
24. Proust A, Matt B, Villanneau T, Guillemot G, Gouzerh P, Izzet G (2012) Chem Soc Rev 41:7605
25. Kato CN, Makino Y, Unno W, Uno H (2013) Dalton Trans 42:1129
26. Raith A, Altmann P, Cokoja M, Herrmann WA, Kühn FE (2010) Coord Chem Rev 254:608
27. Glöckner A, Tamm M (2013) Chem Soc Rev 42:128
28. Krut'ko DP (2009) Russ Chem Bull Int Ed 58:1745
29. Day VW, Earley CW, Klemperer WG, Maltbie DJ (1985) J Am Chem Soc 107:8261
30. Klemperer WG, Zhong B (1993) Inorg Chem 32:5821
31. Radkov EV, Young VG Jr, Beer RH (1999) J Am Chem Soc 121:8953
32. Radkov EV, Beer RH (2000) Inorg Chim Acta 297:191
33. Che TM, Day VW, Francesconi LC, Klemperer WG, Main DJ, Yagasaki A, Yaghi OM (1992) Inorg Chem 31:2920
34. Day VW, Klemperer WG, Maltbie DJ (1985) Organometallics 4:104
35. Tézé A, Hervé G (1977) J Inorg Nucl Chem 39:999
36. Ma R, Wei T, Zhao C (2011) Huaxue Shiji 33:307
37. C.N. Kato, Y. Makino, M. Yamasaki, Y. Kataoka, Y. Kitagawa, M. Okumura, in: Advances in Crystallization Processes, eds. Y. Mastai (InTech, Croatia, 2012) ch.23
38. Weiner H, Aiken JD III, Finke RG (1996) Inorg Chem 35:7905
39. Sheldrick GM (2008) Acta Crystallogr A 64:112
40. Spek AL (2009) Acta Crystallogr D 65:148
41. Brown ID, Altermatt D (1985) Acta Crystallogr B 41:244
42. Brown ID, Shannon RD (1973) Acta Crystallogr A 29:266
43. Brown ID (1992) Acta Crystallogr B 48:553
44. Brown ID (1996) J Appl Crystallogr 29:479
45. Cha JS (2006) Org. Proc. Develop. 10:1032
46. Chuah GK, Jaenicke S, Zhu YZ, Liu SH (2006) Curr Org Chem 10:1639
47. Ishii Y, Nakano T, Inada A, Kishigami Y, Sakurai K, Ogawa M (1986) J Org Chem 51:240
48. Komanoya T, Nakajima K, Kitano M, Hara M (2015) J Phys Chem 119:26540
49. Zhu Y, Jaenick S, Chuah GK (2003) J Catal 218:396
50. Song J, Zhou B, Zhou H, Wu L, Meng Q, Liu Z, Han B (2015) Angew Chem Int Ed 54:9399
51. Li G, Fu WH, Wang YM (2015) Catal Commun 62:10
52. McNerney B, Whittlesey B, Cordes DB, Krempner C (2014) Chem A Eur J 20:14959
53. Mora M, López MI, Jiménez-Sanchidrián C, Ruiz JR (2010) Catal Lett 136:192
54. Ruiz JR, Jiménez-Sanchidrián C, Hidalgo JM, Marinas JM (2006) J Mol Catal A 246:190
55. Shylesha S, Kapoorb MP, Junejab LR, Samuela PP, Srilakshmic C, Singha AP (2009) J Mol Catal 310:118